Fast local warming of sea-surface is the main factor of recent deoxygenation in the Arabian Sea

Zouhair Lachkar, Michael Mehari, Muchamad Al Azhar, Marina Lévy, Shafer Smith

https://doi.org/10.5194/bg-2020-325
Preprint. Discussion started: 14 September 2020

Biogeosciences Discussions

Fast local warming of sea-surface is the main factor of recent deoxygenation in the Arabian Sea

Zouhair Lachkar[1], Michael Mehari[1], Muchamad Al Azhar[1,4], Marina Lévy[2], and Shafer Smith[1,3]

[1]Center for Prototype Climate Modeling, New York University Abu Dhabi, Abu Dhabi, UAE
[2]Sorbonne Université (CNRS/IRD/MNHN), LOCEAN-IPSL, Paris, France
[3]Courant Institute of Mathematical Sciences, New York University, New York, USA
[4]Plymouth Marine Laboratory, Plymouth, UK

Correspondence: Zouhair Lachkar (zouhair.lachkar@nyu.edu)

Abstract.

The Arabian Sea (AS) hosts one of the most intense oxygen minimum zones (OMZs) in the world. Observations show a decline of O_2 in the northern AS over the recent decades accompanied by an intensification of the suboxic conditions there. Over the same period, the local sea-surface temperature has risen significantly, particularly over the Arabian Gulf (also known as Persian Gulf, hereafter the Gulf), while summer monsoon winds have intensified. Here, we reconstruct the evolution of dissolved oxygen in the AS from 1982 through 2010 and explore its controlling factors, with a focus on changing atmospheric conditions. To this end, we use a set of eddy-resolving hindcast simulations forced with observation-based winds and heat and freshwater fluxes. We find a significant deoxygenation in the northern AS with O_2 inventories north of 20°N dropping by over 2% decade^{-1} and 7% decade^{-1} in the top 200 m and the 200-1000 m layer, respectively. These changes cause an increase in the volume of suboxia and the rate of denitrification by 10% decade^{-1} and 13% decade^{-1}, respectively. Using a set of sensitivity simulations we demonstrate that deoxygenation in the northern AS is essentially caused by a reduced ventilation induced by the recent fast warming of the sea surface, in particular in the Gulf. Concomitant summer monsoon wind intensification contributes to deoxygenation at depth and in the upper ocean north of 20°N but enhances oxygenation of the upper ocean elsewhere. This is because surface warming enhances vertical stratification, thus limiting ventilation of the intermediate ocean, while summer monsoon wind intensification causes the thermocline depth to rise in the northern AS and deepen elsewhere, thus contributing to lowering O_2 levels in the upper 200 m in the northern AS and increasing it in the rest of the AS. Our findings confirm that the AS OMZ is strongly sensitive to upper-ocean warming and concurrent changes in the Indian monsoon winds. Finally, our results also demonstrate that changes in the local climatic forcing play a key role in regional dissolved oxygen changes and hence need to be properly represented in global models to reduce uncertainties in future projections of deoxygenation.

1 Introduction

Rising ocean temperatures decrease O_2 solubility in seawater, increase respiration-driven oxygen consumption and enhance vertical stratification, thus reducing interior ocean ventilation (Oschlies et al., 2018). These changes collectively cause the ocean to lose oxygen as it warms up, a process termed ocean deoxygenation. Over the last five to six decades, the global ocean

https://doi.org/10.5194/bg-2020-325
Preprint. Discussion started: 14 September 2020


Biogeosciences Discussions

oxygen content has dropped by 2% (Ito et al., 2017; Schmidtko et al., 2017), a tendency predicted to accelerate in the future in response to ocean warming. Although global models generally misrepresent the observed regional patterns of deoxygenation and underestimate its rate (Oschlies et al., 2018), they all consistently predict further deoxygenation in the future irrespective of the chosen CO_2 emission scenario (Bopp et al., 2013; Cocco et al., 2013). For instance, the Earth system models from the Coupled Model Intercomparison Project Phase 5 (CMIP5) predict a decline of dissolved O_2 of -3.45 $\pm$0.44% by the end of the twenty-first century under the RCP8.5 emission scenario (Bopp et al., 2013). Models from the more recent Coupled Model Intercomparison Project Phase 6 (CMIP6) with generally higher horizontal resolution, more complex biogeochemical models and improved representation of O_2 in the subsurface (Séférian et al., 2020) show a rate of deoxygenation in the 100-600 m subsurface layer that is up to 40% faster than in the CMIP5-based projections (Kwiatkowski et al., 2020). Ocean deoxygenation can cause the expansion of naturally-occurring low-O_2 water bodies known as Oxygen Minimum Zones (OMZs) (Stramma et al., 2008; Breitburg et al., 2018), and has already led to the quadrupling of the volume of anoxic waters since 1960 (Schmidtko et al., 2017). This can increase the frequency and intensity of hypoxic events, stressing sensitive organisms and causing loss of marine biodiversity and shifts in the food web structure (Rabalais et al., 2002; Vaquer-Sunyer and Duarte, 2008; Laffoley and Baxter, 2019). Finally, it has been reported that ocean deoxygenation may cause some oceanic regions to transition to anoxia in the future (Bristow et al., 2017).

The Arabian Sea (AS) hosts one of the world's largest and most extreme OMZs, with suboxia ($O_2 < 4$ mmol m^{-3}) prevailing across most of the intermediate ocean (from 150 down to 1,250 m) in its northern and northeastern parts, turning it in a global hotspot of denitrification (Bange et al., 2005; Codispoti et al., 2001). The previously documented O_2 changes in the AS depict a complex picture with no consistent trends across the entire region (Laffoley and Baxter, 2019). Yet, there is mounting evidence for a decline of O_2 concentrations in the northern and western AS over the last few decades. For example, the global analysis of historical oxygen observations by Ito et al. (2017) reveals a moderate drop of O_2 levels in the subsurface of the AS between 1960 and 2010. The analysis of available O_2 observations by Schmidtko et al. (2017) similarly indicates a decline of oxygen in the northern and western AS as well as along the west coast of India between 1960 and 2010. In an analysis of over 2000 O_2 profiles collected during 53 oceanographic expeditions that took place between 1960 and 2008 off the coast of Oman, Piontkovski and Al-Oufi (2015) documented a decline of O_2 in the upper 300 m in the northern and northwestern AS that they attributed to increased thermal stratification and a shoaling of the oxycline between 1960s and years 2000s. Banse et al. (2014) analyzed discrete historical O_2 measurements collected in the central and southern AS in the 150-500 m layer between 1959 and 2004. They found no clear systematic trend across the entire AS, although O_2 was found to decline in most of the central AS and slightly increase in the southern AS (between 8-12°N). Because of the sparsity of observations, these trends were generally based on small number of samples and not always statistically significant. Authors in this study also analyzed trends in subsurface nitrite (NO_2^-) concentrations, typically used as a proxy of the presence of suboxia and denitrification at depth. They found both positive and negative trends in different locations with a larger number of profiles indicating an increase in nitrite concentrations over time, suggesting an overall intensification of the OMZ over the study period. do Rosário Gomes et al. (2014) reported a radical shift in the winter bloom dominant phytoplankton species from diatoms to large dinoflagellate, Noctiluca scintillans, which they linked to a decline of O_2 concentrations in the region over the

https://doi.org/10.5194/bg-2020-325
Preprint. Discussion started: 14 September 2020


Biogeosciences Discussions Open Access EGU

same period. More recently, using sea glider data and historical observations, Queste et al. (2018) showed an intensification of the suboxic conditions at depth in the Gulf of Oman over the last three decades. Although there has been little work done on documenting potential deoxygenation in the Arabian marginal seas (i.e., the Red Sea and the Gulf), preliminary observations suggest ongoing deoxygenation in the Gulf with recent emergence of summertime hypoxia documented there (Al-Ansari et al., 2015; Al-Yamani and Naqvi, 2019).

In addition to changes in O_2, the AS has undergone several major environmental changes over the recent decades that may intensify in the future. In particular, the AS has experienced a strong warming throughout most of the twentieth century that has accelerated since the early 1990s (Kumar et al., 2009). The warming has been particularly fast in the two Arabian marginal seas (i.e., the Red Sea and the Gulf) over the last three decades with warming rates reaching up to $0.17\pm0.07°C$ decade^{-1} and $0.6\pm0.3°C$ decade^{-1} in the two semi-enclosed seas, respectively (Chaidez et al., 2017; Strong et al., 2011; Al-Rashidi et al., 2009). This is twice to three times faster than the global average. The AS warming has been associated with important ecological and biogeochemical changes. For instance, using satellite observations and a set of historical simulations of the northern Indian Ocean, Roxy et al. (2016) found a drop of summer productivity by up to 20% between 1950 and 2005 in the western AS that they linked to surface warming and increased stratification. Furthermore, the strong Gulf warming has been linked to recent frequent mass coral bleaching events there (Burt et al., 2019). Additionally, using a set of idealized model simulations, Lachkar et al. (2019) found the warming of the Gulf to induce a reduction of the ventilation of the AS OMZ, thus causing its intensification. Important changes in the regional monsoon winds have also been reported. For instance, Goes et al. (2005) have documented an increase in summer monsoon wind intensity off Somalia between 1997 and 2005. Other studies have also suggested a climate change driven intensification of the summer monsoon winds (Wang et al., 2013) and weakening of winter monsoon winds (Parvathi et al., 2017) in the northern AS. Finally, Lachkar et al. (2018) found a tight link between the strength of the monsoon winds and the depth and intensity of the AS OMZ.

While these environmental perturbations may have contributed to the observed O_2 decline over the recent decades, their potential interactions and the mechanisms through which they act to modulate O_2 remain largely poorly understood. In particular, the respective roles of recent surface warming on the one hand and summer monsoon wind intensification on the other hand are yet to be quantified. Moreover, the potential contribution of the recent fast warming of the Gulf to the declining O_2 levels in the northern AS has not yet been investigated. Here we reconstruct the trends in O_2 over the period between 1982 and 2010 using a high-resolution hindcast simulation of the Indian Ocean and examine their physical and biogeochemical drivers using a set of sensitivity experiments. We show that recent deoxygenation in the northern AS has been caused essentially by surface warming, in particular in the Gulf, bringing about a reduction in the ventilation of the subsurface and intermediate layers. We also show that summer monsoon intensification enhanced oxygenation of the upper ocean south of 20°N but has contributed to deoxygenation in the northern AS. These changes are likely to have important ecological and biogeochemical consequences.

https://doi.org/10.5194/bg-2020-325
Preprint. Discussion started: 14 September 2020


Biogeosciences Discussions

2 Methods

2.1 Models

The circulation model is the Regional Ocean Modeling System (ROMS)-AGRIF version (http://www.croco-ocean.org) configured for the Indian Ocean. It uses the free-surface, hydrostatic, primitive equations in a rotating environment and has a terrain-following vertical coordinate system (Shchepetkin and McWilliams, 2005). To limit diapycnal mixing errors, the diffusive component of the rotated, split, upstream-biased, 3rd order (RSUP3) tracer advection scheme is rotated along geopotential surfaces (Marchesiello et al., 2009). The non-local K-Profile Parameterization (KPP) scheme is used to parametrize subgrid vertical mixing (Large et al., 1994). The model domain covers the full Indian Ocean from 31°S to 31°N and 30°E to 120°E with a 1/10° horizontal resolution and 32 sigma-coordinate vertical layers with enhanced resolution near the surface. The biogeochemical model is a nitrogen-based nutrient-phytoplankton-zooplankton-detritus (NPZD) model (Gruber et al., 2006). It is based on a system of ordinary differential equations representing the time-evolution of seven state variables: two nutrients (nitrate and ammonium), one phytoplankton class, one zooplankton class, two classes of detritus (small and large sizes) and a dynamic chlorophyll-to-carbon ratio. The model has a module describing the cycling of oxygen as well as a parameterization of water-column and benthic denitrification (Lachkar et al., 2016).

2.2 Experimental design

The hindcast simulation is forced with ECMWF ERA-Interim 6-hourly heat fluxes, air temperature, pressure, humidity, precipitation and winds over the period from January 1982 to December 2010. Sea surface temperature is restored to AVHRR-Pathfinder and Aqua-Modis observations and surface salinity is restored to the Simple Ocean Data Assimilation (SODA) reanalysis data using kinematic heat and freshwater flux corrections proposed by Barnier et al. (1995). Initial and lateral boundary conditions for temperature, salinity, currents and sea surface height are computed from the SODA reanalysis. The initial and lateral boundary conditions for nitrate and oxygen are extracted from the World Ocean Atlas (WOA) 2013 (Garcia et al., 2013a, b). Finally, we used a monthly climatological runoff and annual river nutrient discharge from major rivers in the northern Indian Ocean derived from available observations and a global hydrological model (Ramesh et al., 1995; Dai and Trenberth, 2002; Krishna et al., 2016). We restrict our analysis to the AS region extending from 5°S to 30°N in latitude and from 32°E to 78°W in longitude (Fig S1, Supporting Information (SI)).

The model is spun-up using climatological forcing during 58 years and is then run for four 29-year (1982-2010) repeating forcing cycles, with the first three cycles used as a part of the spin-up period (i.e., the total duration of the spin-up phase is 145 years) and the forth cycle used for analysis (similar to the forcing protocol used in the Ocean Model Intercomparison Project, Griffies et al., 2016). The climatological run is extended for an additional 29 years to quantify the artificial trends purely driven by the model drift and contrast them to trends estimated in our hindcast run. The analysis of model drift indicates a very negligible drift in salinity by the end of the climatological forcing period (Fig S2). For O_2, the model drift decreases but remains positive (ocean oxygenation) by the end of the climatological forcing spin-up period, suggesting that the estimated

https://doi.org/10.5194/bg-2020-325
Preprint. Discussion started: 14 September 2020

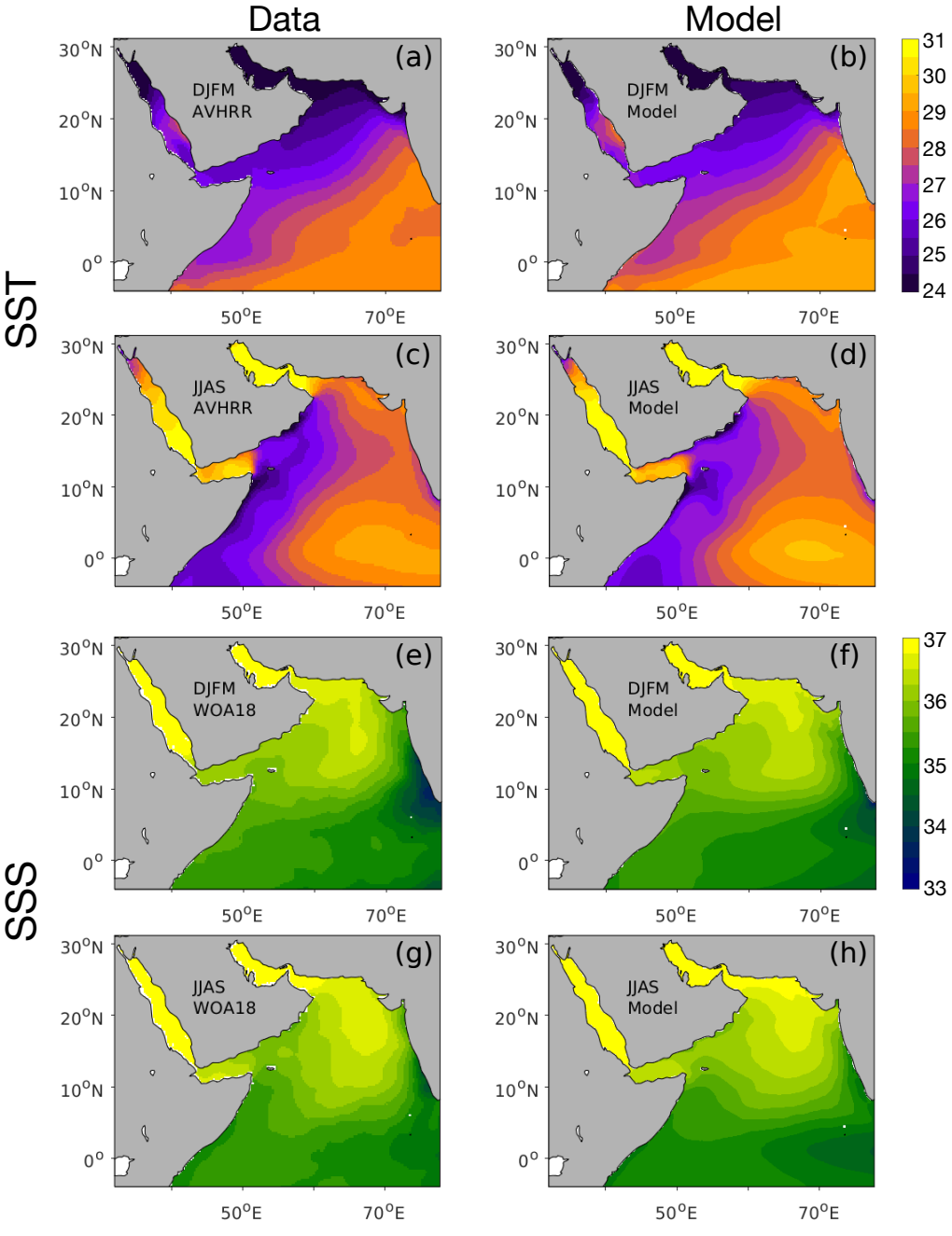

Figure 1. Evaluation of model simulated sea surface temperature and salinity (a-d) Sea surface temperature (in °C) as simulated in the model (right) and from the AVHRR satellite product (left) in winter (top) and summer (bottom) monsoon seasons.(e-h) Sea surface salinity (in PSU) as simulated in the model (right) and from the WOA-2018 dataset (left) in winter (top) and summer (bottom) monsoon seasons.

https://doi.org/10.5194/bg-2020-325
Preprint. Discussion started: 14 September 2020

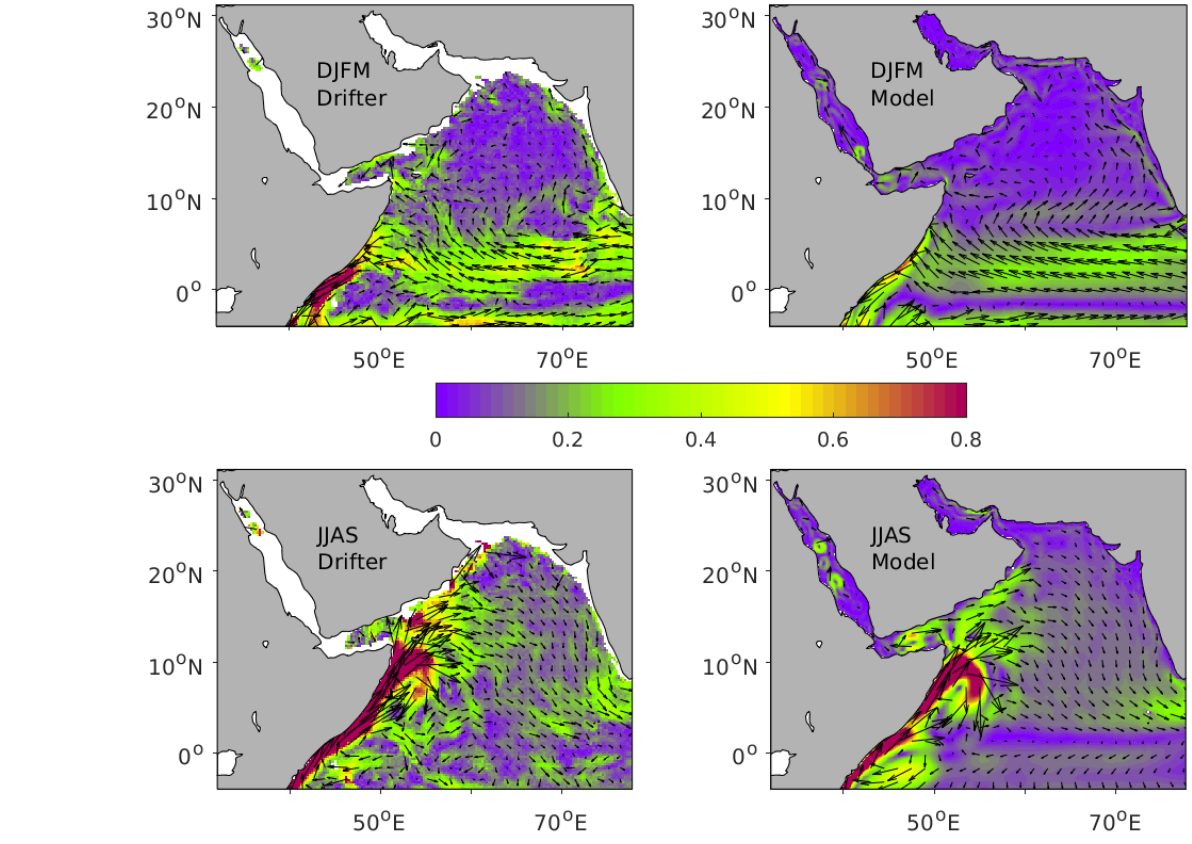

Figure 2. Evaluation of model simulated surface currents Surface currents (in $m\,s^{-1}$) as simulated in the model (right) and from surface drifter climatology of Lumpkin and Johnson (2013) (left) during winter (top) and summer (bottom) monsoon seasons.

deoxygenation rates extracted from our hidncast simulation are rather conservative (Figs S2-S5, SI). A detailed description of the model drift is presented in the SI.

2.3 Model evaluation

We use available in-situ and satellite-based observations to evaluate the performance of the model in capturing the spatial and seasonal variability in key physical and biogeochemical properties. We first evaluate the mean state by contrasting a model climatology computed over the (1982-2010) study period to available observation-based climatologies.

The model reproduces well the observed distributions of sea surface temperature (SST) inferred from the Advanced Very High Resolution Radiometer (AVHRR) satellite data in both winter and summer seasons (Fig 1). In particular, the model captures the intense temperature gradients prevailing in both seasons across the AS. Indeed, the model reproduces the strong temperature contrasts between the AS and its marginal seas, i.e., the Gulf and the Red Sea as well as the upwelling-driven cold SST tongue that develops in the west AS during summer. Similarly, the distribution of the mean surface salinity is in a

https://doi.org/10.5194/bg-2020-325
Preprint. Discussion started: 14 September 2020

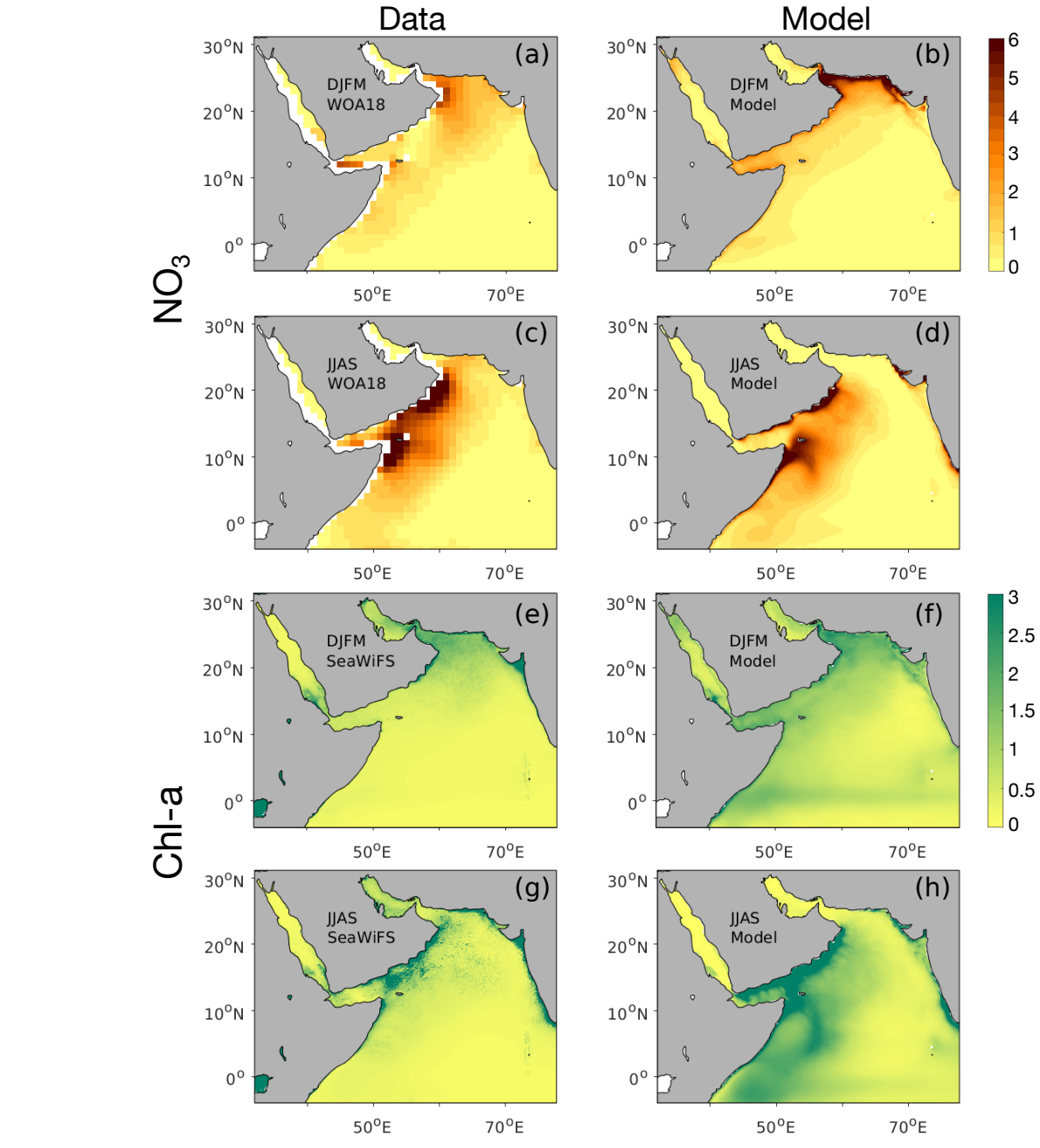

Figure 3. Evaluation of model simulated surface nitrate and chlorophyll-a (a-d) Surface NO_3^- (in mmol m^{-3}) as simulated in the model (right) and from the WOA-2018 dataset (left) in winter (top) and summer (bottom) monsoon seasons. (e-h) Sea surface chlorophyll-a concentrations (in mg m^{-3}) as simulated in the model (right) and from SeaWiFS climatology (left) during winter (top) and summer (bottom) monsoon seasons.

https://doi.org/10.5194/bg-2020-325
Preprint. Discussion started: 14 September 2020

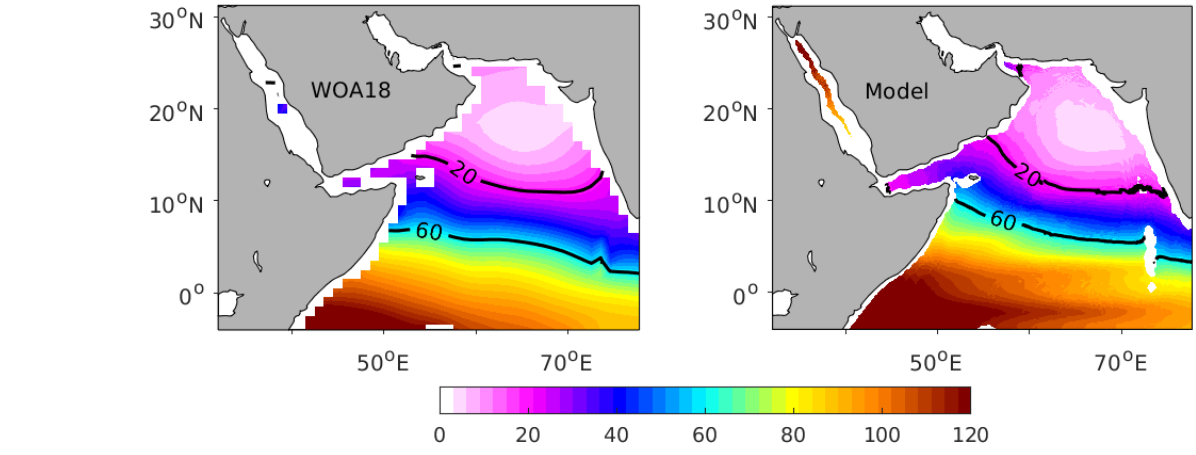

Figure 4. Evaluation of model simulated oxygen Annual mean O_2 averaged between 250 m and 700 m (in mmol m^{-3}) as simulated in the model (right) and from the WOA-2018 dataset (left).

good agreement with that from the WOA2018 climatology (Fig 1). The AS surface circulation is similarly well represented in the model in both summer and winter seasons (Fig 2). In particular, the model simulates well the reversal of the Somali Current between summer and winter seasons as well as the prominent features of the surface circulation system including the Southern Gyre, the Great Whirl and the Southwest Monsoon Current in summer and the Northeast Monsoon Current and South Equatorial Countercurrent in winter (Schott et al., 2009).

The model reproduces relatively well the observed surface distribution of nitrate in both seasons, despite a tendency towards slightly overestimating surface concentrations in the oligotrophic open ocean and underestimating them in the northern AS during summer (Fig 3). The large-scale nitrate distribution at depth is also well captured by the model despite some local biases (Fig S6, SI). The model reproduces the observed high chlorophyll-a concentrations associated with the winter and summer blooms in the northern and western AS, respectively (Fig 3). Furthermore, summer high chlorophyll concentrations off the Indian west coast are also relatively well captured by the model. In contrast, the model tends to substantially overestimate chlorophyll levels off the Somali coast and in the western AS in general. This discrepancy may result from the fact that the model does not represent iron and silicic acid that may be contributing to limiting productivity in this region (Koné et al., 2009). Finally, the model captures fairly well the large-scale distribution of oxygen in the AS region (Fig 4). In particular, the location, size and intensity of the AS oxygen minimum zone is relatively well reproduced.

A more quantitative assessment of the model performance is shown using Taylor diagrams (Taylor, 2001) that summarize three important statistics: (i) the correlation coefficient between the model and the observations, (ii) the standard deviation in the model relative to the observations and (iii) the centered root mean square (RMS) with respect to observations (Fig 5). To this end, in-situ observations from the World Ocean Database (2018) were binned temporally and spatially into a 0.5° x 0.5° seasonal climatology covering the AS region. No spatial interpolation was performed and the model and observations are contrasted at the observation points only. This analysis confirms the relatively good agreement between model and observations.

https://doi.org/10.5194/bg-2020-325
Preprint. Discussion started: 14 September 2020

More specifically, it shows that surface temperature and salinity, as well as upper (400 m) ocean nitrate and O_2 distributions generally all agree well with observations with correlations above 0.9 and comparable standard deviations, across all seasons (Fig 5). The model shows a weaker performance though in simulating surface chlorophyll with correlations ranging from 0.42 during winter months to 0.67 during the Fall season (Fig 5).

Finally, we evaluate the model performance in reproducing observed long term changes. To this end, we binned observations from the World Ocean Database (2018) seasonally on a 5° x 5° horizontal grid at each standard depth. We then computed seasonal climatologies for the first five years (1982-1986) and the last five years (2006-2010) for each bin where at least three observations were available from each year in the two periods. Using these requirements allows us to reduce the local noise in the estimated long-term changes. Yet, only temperature was found to have a coverage that is sufficiently dense to enable these anomalies to be estimated over a significant portion of the AS. Contrasting the long term temperature changes in the top 200 m in the model and in the observations reveals an overall good agreement in terms of the magnitude and the patterns of upper ocean warming in both summer and winter seasons (Fig S7 and Fig S8, SI).

In summary, despite a few identified biases, the model exhibits reasonable skill in reproducing the mean seasonal climatological state for both physical and biogeochemical properties. Furthermore, it reproduces fairly well the structure and intensity of the AS oxygen minimum zone. Finally, both the magnitude and patterns of the simulated upper ocean warming are consistent with observations.

3 Results

3.1 Deoxygenation trends in the Arabian Sea

To investigate long-term changes in O_2 time series, data was deseasonalized by removing monthly climatologies from the original time series. Furthermore, to identify significant trends in O_2 we used the non-parametric Mann-Kendall (MK) test (Mann, 1945; Kendall, 1948) that does not assume normality of data distribution and hence is less sensitive to outliers and skewed distributions. The analysis of oxygen trends between 1982 and 2010 shows a decline of O_2 concentrations in the northern and western AS in the upper 200 m (Fig. 6a). Below 200 m, the drop in O_2 is particularly important in relative terms in the northern AS but other areas in the southern and southeastern AS also show negative trends although with a weaker magnitude (Fig. 6b). A vertical transect at 65°E indicates that in absolute terms most of the O_2 decline is concentrated north of 20°N in the top 300 m (Fig. 6c). This deoxygenation results in a significant intensification of the OMZ over the three decade study period, with the volume of suboxic ($O_2 < 4 \mathrm{mmol\,m^{-3}}$) water increasing by nearly 10% per decade (Fig. 7a). This causes an amplification of denitrification in the region with an increase in denitrification rates by around 14% per decade over the same period (Fig. 7c). Despite deoxygenation trends dominating in the northern and western AS, local oxygenation patches are simulated in the eastern, central and southern AS (Fig 6). This results in the net hypoxic volume ($O_2 < 60\ \mathrm{mmol\,m^{-3}}$) to change little over the study period (Fig 7b). Next, we focus on the northern AS (north of 20°N) where simulated deoxygenation and its impacts on the OMZ are the most prominent.

https://doi.org/10.5194/bg-2020-325
Preprint. Discussion started: 14 September 2020

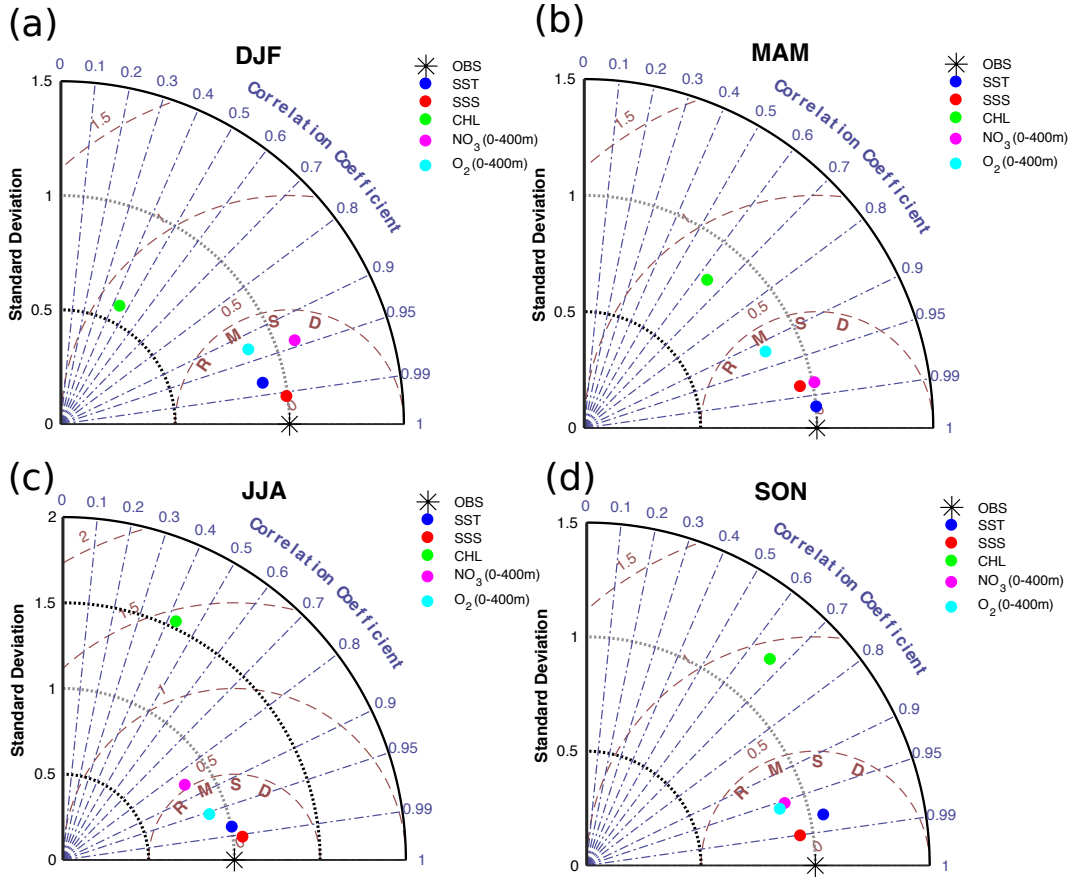

Figure 5. Model skill assessment with Taylor diagrams. Taylor diagram presenting statistical comparison of modeled and observed variables. Taylor (2001) diagram of sea surface temperature (blue), salinity (red), chlorophyll-a (green) and nitrate (purple) and oxygen (cyan) in the upper 400 m in (a) winter, (b) spring, (c) summer and (d) fall. The reference point in the Taylor diagram corresponds to observations. The radius (distance to the origin point) represents the modeled standard deviation relative to the standard deviation of the observations. The angle between the model point and the X-axis indicates the correlation coefficient between the model and the observations. Finally, the distance from the reference point to a given modeled field represents that field's centered root mean square (RMS) with respect to observations.

3.2 Drivers of ocean deoxygenation

In the northern AS (north of 20°N), oxygen inventory drops by nearly 2.2% per decade and up to 7% per decade in the upper 200 m and between 200 and 1000 m, respectively (Fig. 8b and Fig. 8c). We found these trends to be statistically significant at 95% confidence interval in both layers. The decline of O_2 near the surface (top 30 m) is weaker in relative terms (-0.35% decade^{-1}) and is predominantly (over 70%) driven by a drop in O_2 saturation associated with decreasing solubility (Fig 8a). Yet, deoxygenation trends in the thermocline (0-200 m) and in the ocean interior (200-1000 m) seem to emerge mostly from

https://doi.org/10.5194/bg-2020-325
Preprint. Discussion started: 14 September 2020

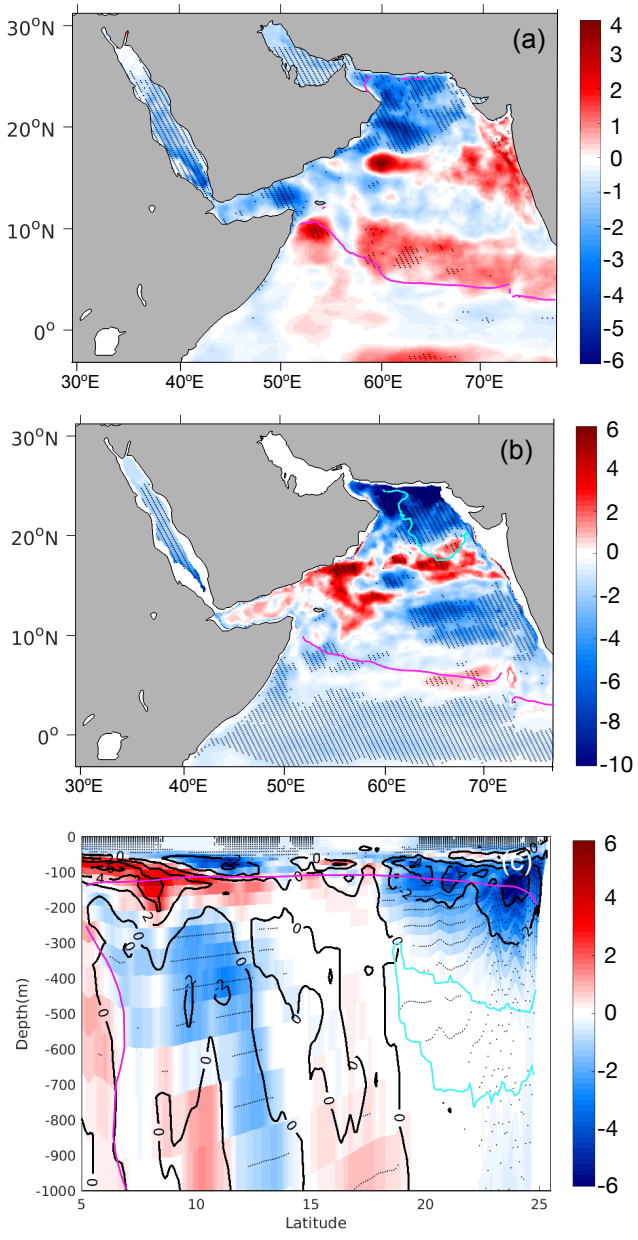

Figure 6. Deoxygenation rates in the AS between 1982 and 2010. (a-b) Trends in O_2 inventories (in % per decade) in (a) the top 200 m and (b) the 200-1000 m layer. (c) trends in O_2 in the upper 1000 m across 65°E (in mmol m^{-3} $decade^{-1}$). Statistically significant trends at 95% confidence interval following a Mann-Kendall (MK) test are represented by hatching (a-b) and stippling (c). The purple and cyan lines indicate the average positions of the hypoxic ($O_2 < 60$ mmol m^{-3}) and suboxic ($O_2 < 4$ mmol m^{-3}) boundaries, respectively, (a) at 100 m, (b) 500 m and (c) along 65°E.

https://doi.org/10.5194/bg-2020-325
Preprint. Discussion started: 14 September 2020

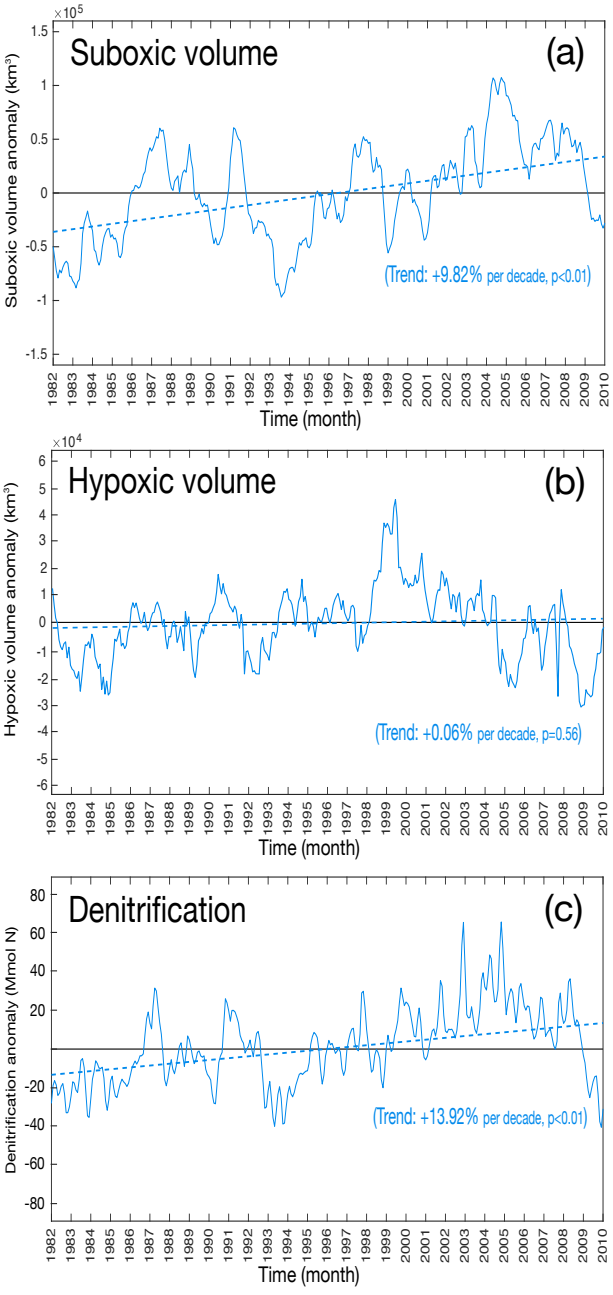

Figure 7. Changes in Oxygen Minimum Zone intensity and denitrification. Interannual anomalies in the volume of (a) suboxia (b) hypoxia and (c) water column denitrification over the study period. The dashed lines indicate the trend lines.

https://doi.org/10.5194/bg-2020-325
Preprint. Discussion started: 14 September 2020

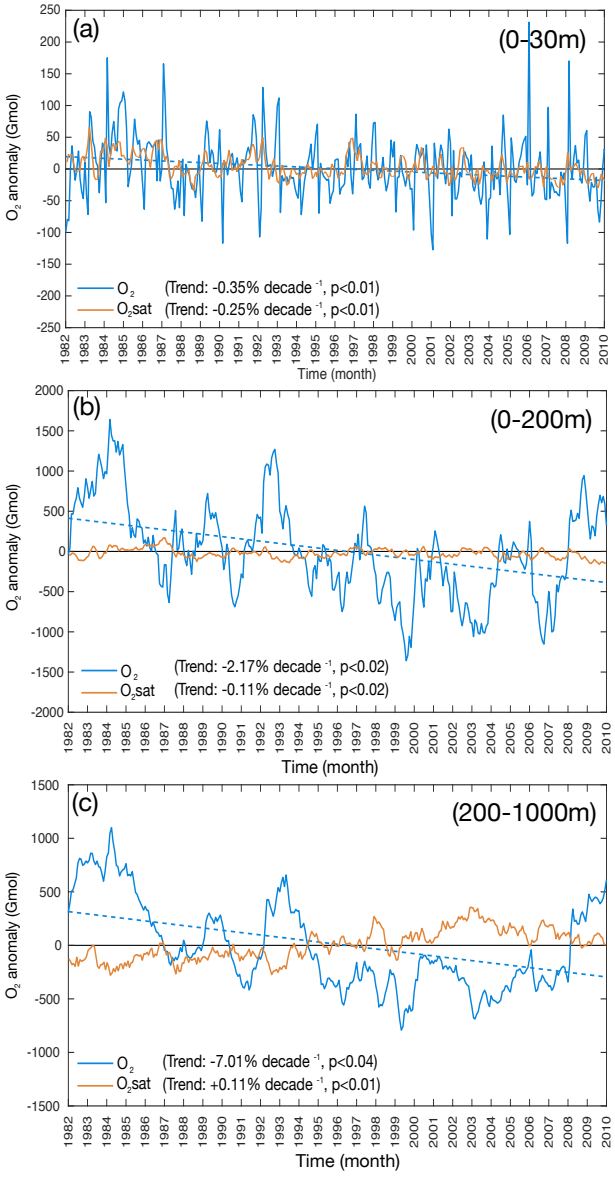

Figure 8. Drivers of northern AS deoxygenation between 1982 and 2010. O_2 content (blue) and O_2 saturation (orange) anomalies in (a) the top 30 m, (b) the top 200 m and (c) the 200-1000 m layer as a function of time. The blue dashed line indicates the trend line in O_2 inventory in each layer.

https://doi.org/10.5194/bg-2020-325
Preprint. Discussion started: 14 September 2020


Biogeosciences Discussions

changes in the apparent oxygen utilization (AOU) as O_2 saturation declines very weakly in the upper 200 m and even slightly increases below 200 m during the study period (Fig. 8b and Fig. 8c).

To further explore the drivers of ocean deoxygenation in the northern AS, we performed an O_2 budget analysis north of 20°N in the 100-200 m and the 200-1000 m layers (Fig. 9). To this end, we quantified the cumulative O_2 anomalies in each of the two vertical layers and calculated the respective contributions of transport and biology to these. In order to explain changes in O_2 that are consistent with the identified linear trends, we run this budget between the first (beginning of 1982) and the last (beginning of 2008) intersection of O_2 time series with the trend line. This analysis indicates that most of O_2 decline in the upper 200 m of the northern region is associated with a drop in ventilation, with little contribution from changes in biological consumption (Fig. 9a). Below 200 m, the increase in biological consumption slightly contributes to the deoxygenation trends, but ventilation reduction still dominates both interannual variability and long-term trends in O_2 (Fig. 9b). Splitting the ventilation contribution into lateral and vertical components reveals that the decline in O_2 in the upper 200 m is primarily caused by a reduction in vertical ventilation, whereas below 200 m deoxygenation is more driven by reduced lateral O_2 supply (Fig S9, SI). Next, we explore the changes in physical forcing causing these trends.

3.3 Impact of changes in atmospheric forcing

The analysis of long-term trends in atmospheric forcing reveals a widespread warming of the sea surface by between 0.5 and 1°C in the northern AS and by up to 1.5°C in the Gulf and in the northern part of the Red Sea, between 1982 and 2010 (Fig 10a). In addition to surface warming, surface winds have undergone important changes with an intensification of upwelling favorable winds off Somalia and Oman, in particular during the summer monsoon season (Fig 10b and Fig S10, SI).

To quantify the contributions of surface warming and wind changes to northern AS deoxygenation, we performed three additional sensitivity experiments. In the first simulation, S_{hclim}, all atmospheric and lateral boundary conditions were set to vary interannually like in the control run except the heat fluxes that were extracted from a normal year, 1986, and repeated every year (i.e., climatological heat fluxes). In the second sensitivity run, S_{hclim_AG}, the heat fluxes were similarly extracted from year 1986 and repeated annually, but only over the Gulf region (i.e., climatological heat fluxes over the Gulf only). Finally, in a third simulation S_{wclim_JJAS} all atmospheric and lateral boundary conditions were set to vary interannually like in the control run except summer monsoon winds that were extracted from the year 1986 and repeated every year (i.e., climatological summer winds). By comparing S_{hclim} to the control, we can quantify the role of surface warming over the entire domain on deoxygenation. Similarly, contrasting S_{hclim_AG} with the control run allows us to measure the relative importance of the fast warming of the Gulf on the deoxygenation in the northern AS. Finally, by comparing S_{wclim_JJAS} to the control we can quantify the role of summer monsoon wind changes in the simulated deoxygenation.

Under climatological heat fluxes, oxygen increases in most of the AS in the upper 200 m, with the oxygen inventory north of 20°N increasing by nearly 1.6% between 1982 and 2010 (Fig 11). Below 200 m, O_2 strongly increases in the northern AS by nearly 7% over the study period (Fig 11). Contrasting these oxygenation trends with the strong deoxygenation simulated in the control suggests that surface warming is the main cause of deoxygenation in the northern AS (Fig S11, SI). When the heat fluxes are set to be climatological over the Gulf region only, oxygen decreases in the northern AS both in the top 200 m and

https://doi.org/10.5194/bg-2020-325
Preprint. Discussion started: 14 September 2020

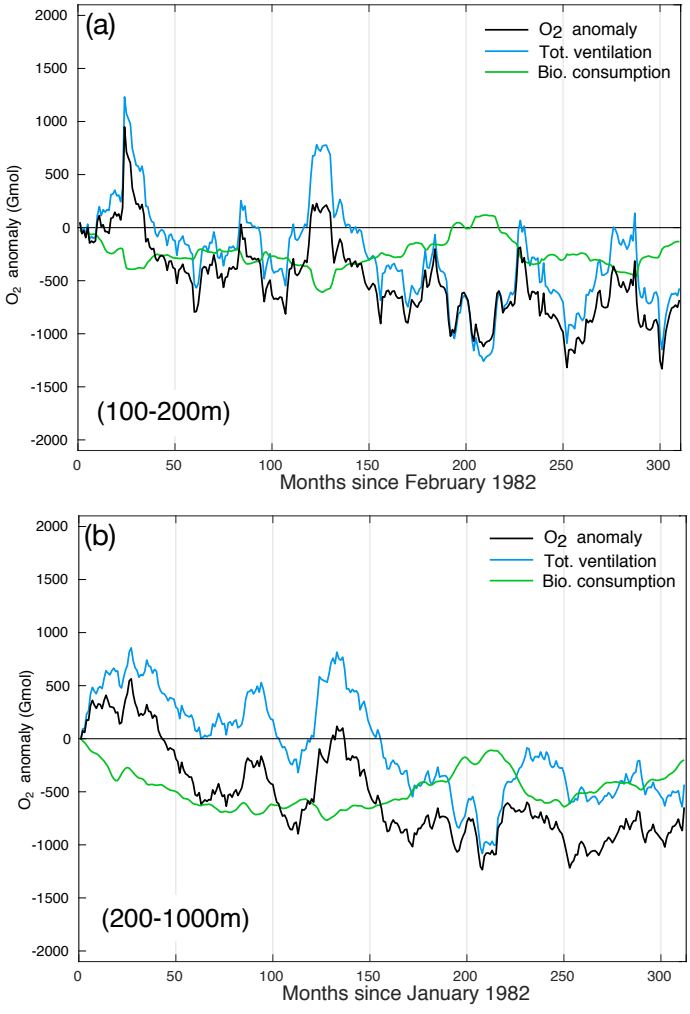

Figure 9. Role of ventilation and biology in AS deoxygenation. Cumulative O_2 anomalies (black) and their biological (green) and physical (blue) sources in (c) the (100-200m) subsurface and (d) the intermediate (200-1000m) ocean.

between 200 and 1000 m, but deoxygenation rates are nearly twice (0-200 m) to five times (200-1000 m) weaker than in the control (Fig 11 and Fig S11, SI). This indicates that the fast warming over the Gulf has likely contributed to the northern AS recent strong deoxygenation. Finally, in the absence of interannual changes in summer winds, simulated deoxygenation rates in the northern AS are weaker than in the control simulation (Fig 11). However, deoxygenation trends become stronger in most of the rest of the AS in the top 200 m and in the central and eastern AS below 200 m (Fig 11 and Fig S11, SI). This suggests that summer upwelling intensification contributes to deoxygenation in the northern AS and in the western AS at depth but acts to oxygenate the upper ocean in the rest of the AS.

In summary, we conclude that deoxygenation in the northern AS is essentially caused by surface warming and that the fast warming of the Gulf plays an important role in this trend. Summer monsoon intensification contributes to deoxygenation in

https://doi.org/10.5194/bg-2020-325
Preprint. Discussion started: 14 September 2020

Biogeosciences Discussions Open Access EGU

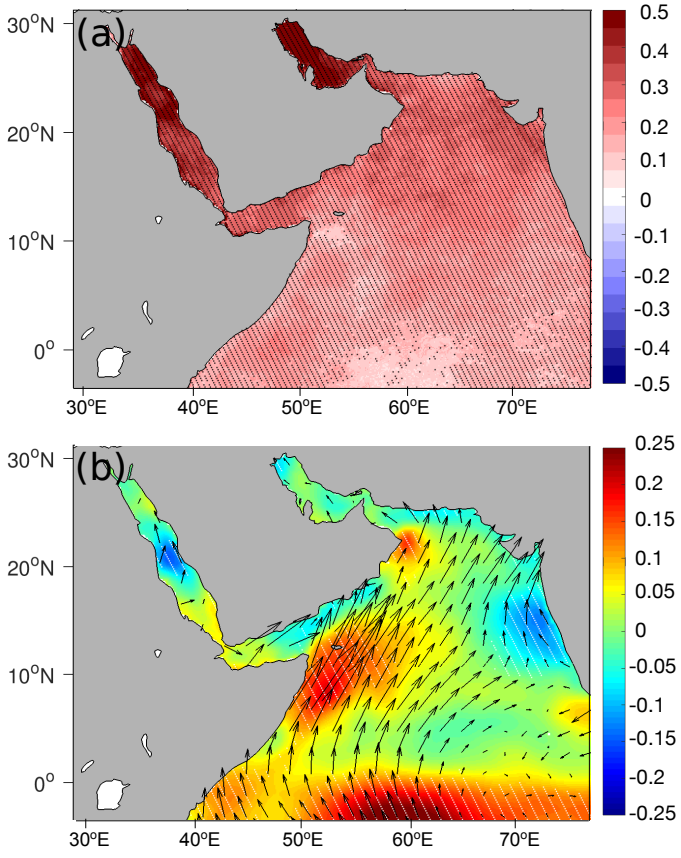

Figure 10. Warming and surface wind changes. Linear trends in (a) sea surface temperature (in °C per decade) and (b) surface winds (color shading indicates trends in wind speed (in m s^{-1} $decade^{-1}$) whereas arrows show trends in wind stress vector). Statistically significant trends at 95% confidence interval following a Mann-Kendall (MK) test are represented by hatching.

the northern AS as well as in the western AS at depth. However, increasing summer winds do also enhance the oxygenation of the upper ocean south of 20°N. Next, we explore the mechanisms through which surface warming and enhanced summer monsoon winds cause these oxygen trends.

3.4 Mechanisms of Arabian sea reduced ventilation

The strong surface warming resulted in an increase in vertical stratification that is particularly important in the northern AS with stratification at 200 m increasing on average by nearly 4% per decade (Fig 12a and Fig S12a, SI). This likely contributes to the reduction in the vertical ventilation in the upper ocean as revealed by our O_2 budget analysis (Fig S9, SI). Under climatological heat fluxes, upper ocean stratification does decrease in most of the AS, and in particular in the northern AS (Fig 12c and Fig S12, SI). This confirms that most of the increase in vertical stratification in the control simulation is caused by surface warming (Fig S13a, SI).

https://doi.org/10.5194/bg-2020-325
Preprint. Discussion started: 14 September 2020

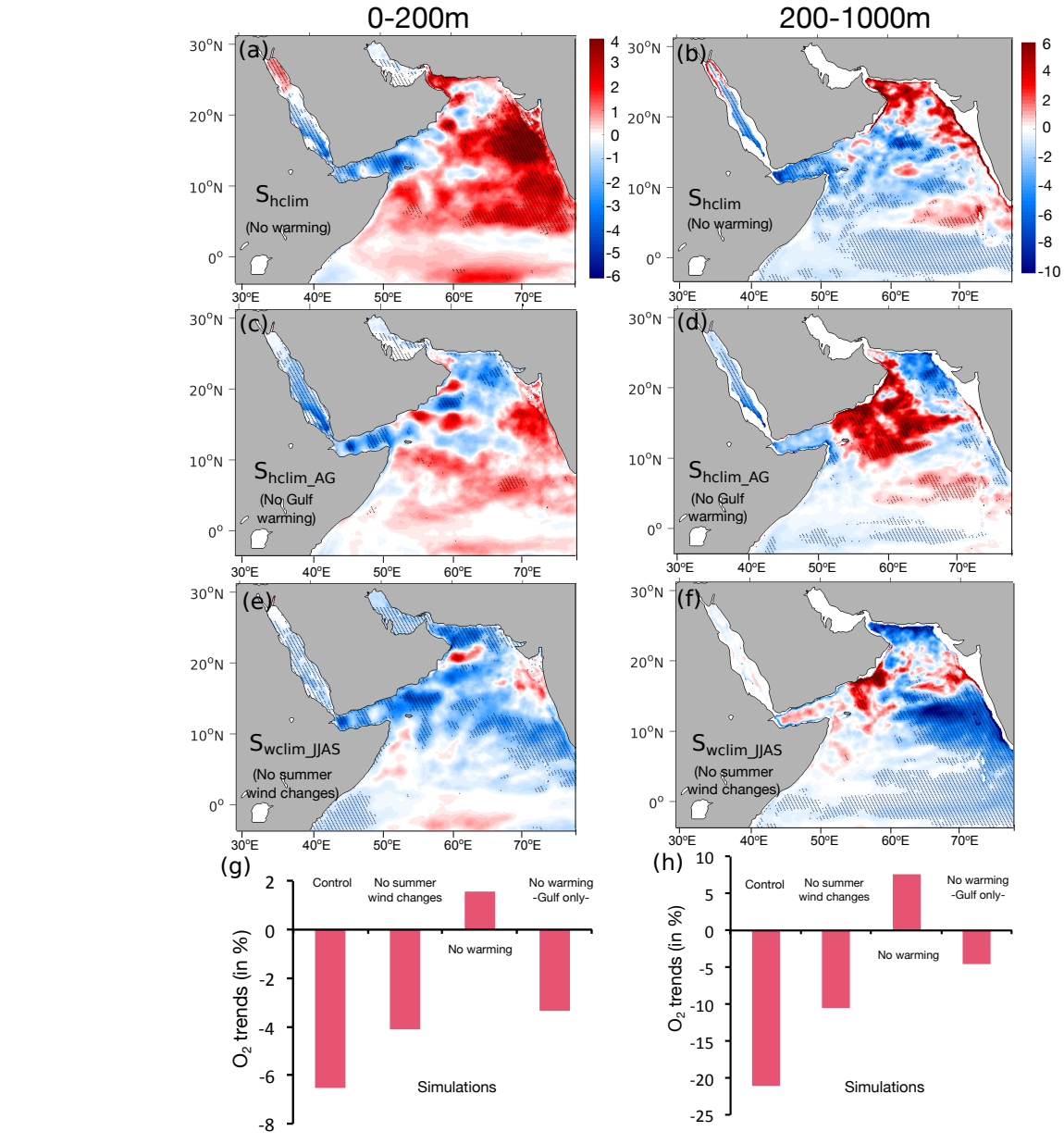

Figure 11. Deoxygenation rates under different atmospheric forcing scenarios. Linear trends in O_2 inventories (left) in the top 200 m and (right) in the 200-1000 m layer (in % per decade) in the (a-b) S_{hclim} (no warming), (c-d) S_{hclim_AG} (no Gulf warming) and (e-f) S_{wclim_JJAS} (no summer wind changes) simulations. (g-h) Trends in O_2 (in %) in the northern AS (north of 20°N) in the control and under different forcing scenarios in (g) the top 200 m and (h) the 200-1000 m layer. Statistically significant trends at 95% confidence interval following a Mann-Kendall (MK) test are represented by hatching.

https://doi.org/10.5194/bg-2020-325
Preprint. Discussion started: 14 September 2020

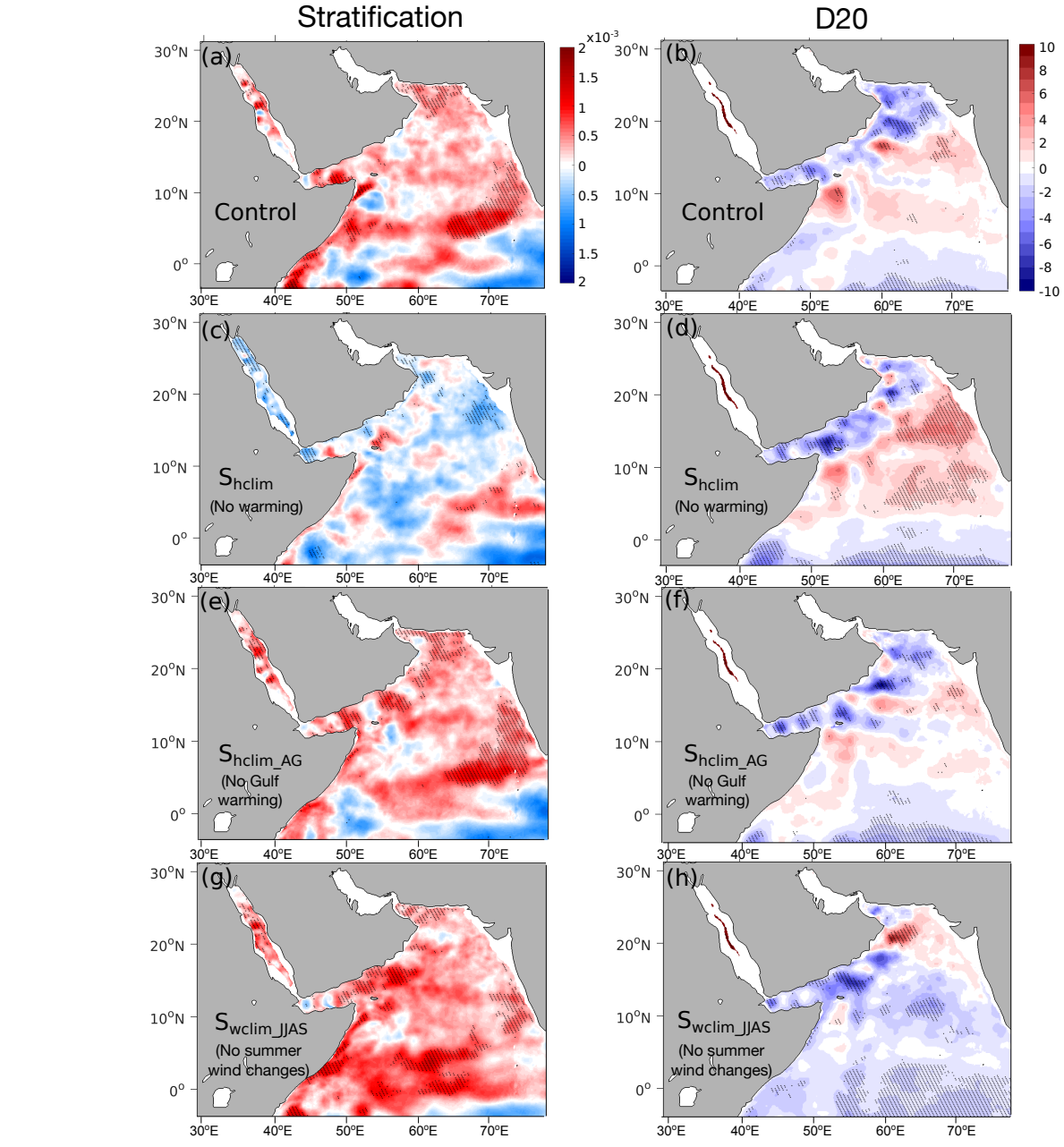

Figure 12. Vertical stratification and thermocline depth under different atmospheric forcing scenarios. Linear trends in (left) vertical stratification (in $g\,m^{-4}$ $decade^{-1}$) and (right) depth of isotherm 20°C D20 (in $m\,decade^{-1}$) in the (a-b) control and (c-h) under different atmospheric forcing scenarios. Statistically significant trends at 95% confidence interval following a Mann-Kendall (MK) test are represented by hatching.

https://doi.org/10.5194/bg-2020-325
Preprint. Discussion started: 14 September 2020

When the heat fluxes are set to be climatological over the Gulf only, the increase in vertical stratification is similar to that in the control run over most of the AS, including the region north of 20°N (Fig S12 and Fig S12, SI). This suggests that the reduction in the ventilation of the northern AS is not entirely caused by enhanced vertical stratification and that other mechanisms are likely at play. Lachkar et al. (2019) have shown that the AS OMZ can intensify in response to strong warming of the Gulf causing a reduced outflow of the Gulf water in the northern AS. Here, we find the depth of the Gulf water has shoaled locally by up to 20 m in the Gulf of Oman in the control run relative to the S_{hclim_AG} run (Fig S14, SI).

Finally, the summer monsoon wind intensification is likely to affect upper ocean mixing and thermocline depth, and hence vertical ventilation and oxygen levels in the upper ocean. Furthermore, changes in summer monsoon winds can also affect upwelling off Somalia and Oman and hence alter productivity and O_2 consumption at depth in the western AS, potentially impacting O_2 supply to northern AS. The analysis of trends in thermocline depth, typically represented by the depth of isotherm 20°C in the tropical Indian Ocean (e.g. Schott et al., 2009), reveals a shoaling of this interface in the western and northern AS by up to 6 m per decade and a slight deepening in the central and eastern AS (Fig 12b). In contrast, under climatological summer monsoon winds the themocline depth shoals almost everywhere in the AS except in the northern region where a deepening is observed (Fig 12h). This suggests that summer monsoon wind intensification cause the thermocline depth to rise in the northern AS and deepen elsewhere (Fig S15c, SI). The shoaling of the thermocline depth contributes to lowering O_2 levels in the upper 200 m in the northern AS whereas its deepening south of 20°N contributes to increase O_2 levels in the top 200 m. Increased summer monsoon winds increase biological productivity in the western and central AS by up to 5% per decade in the control run (Fig 13). In contrast, productivity shows a limited increase or even a decrease in the western AS under climatological summer winds (Fig 13). The enhancement in productivity south of 20°N that results from summer monsoon wind intensification is associated with an increase in O_2 consumption (hence a decrease in O_2) at depth in the central and western AS (Fig S16c and Fig S17c, SI). This contributes to deoxygenation observed at depth in the central and western AS. The lower O_2 levels in the central and western AS are likely contributing to the reduced O_2 supply to the northern AS (Fig S9b, SI) as meridional circulation shows little change over the study period (Fig S18, SI).

4 Discussion

4.1 Role of biology

The relatively limited role of biology in the northern AS deoxygenation is a direct consequence of the minimal change the biological productivity has experienced in the region over the study period as well as due to the negative feedback of enhanced denitrification on O_2 consumption at depth. Indeed, the biological productivity has changed little in the northern AS as enhanced stratification on the one hand and increased summer upwelling on the other hand have opposing effects on nutrient supply to the euphotic zone. For instance, productivity increases substantially in the northern AS and across the domain in the absence of surface warming (Fig 13). Conversely, under climatological summer winds productivity tends to decrease in most of the northern and western AS (Fig 13). Finally, the enhanced denitrification associated with the deoxygenation trends reduces aerobic O_2 consumption and hence opposes deoxygenation in the northern AS (Fig S19, SI).

https://doi.org/10.5194/bg-2020-325
Preprint. Discussion started: 14 September 2020

Biogeosciences
Discussions
Open Access
EGU

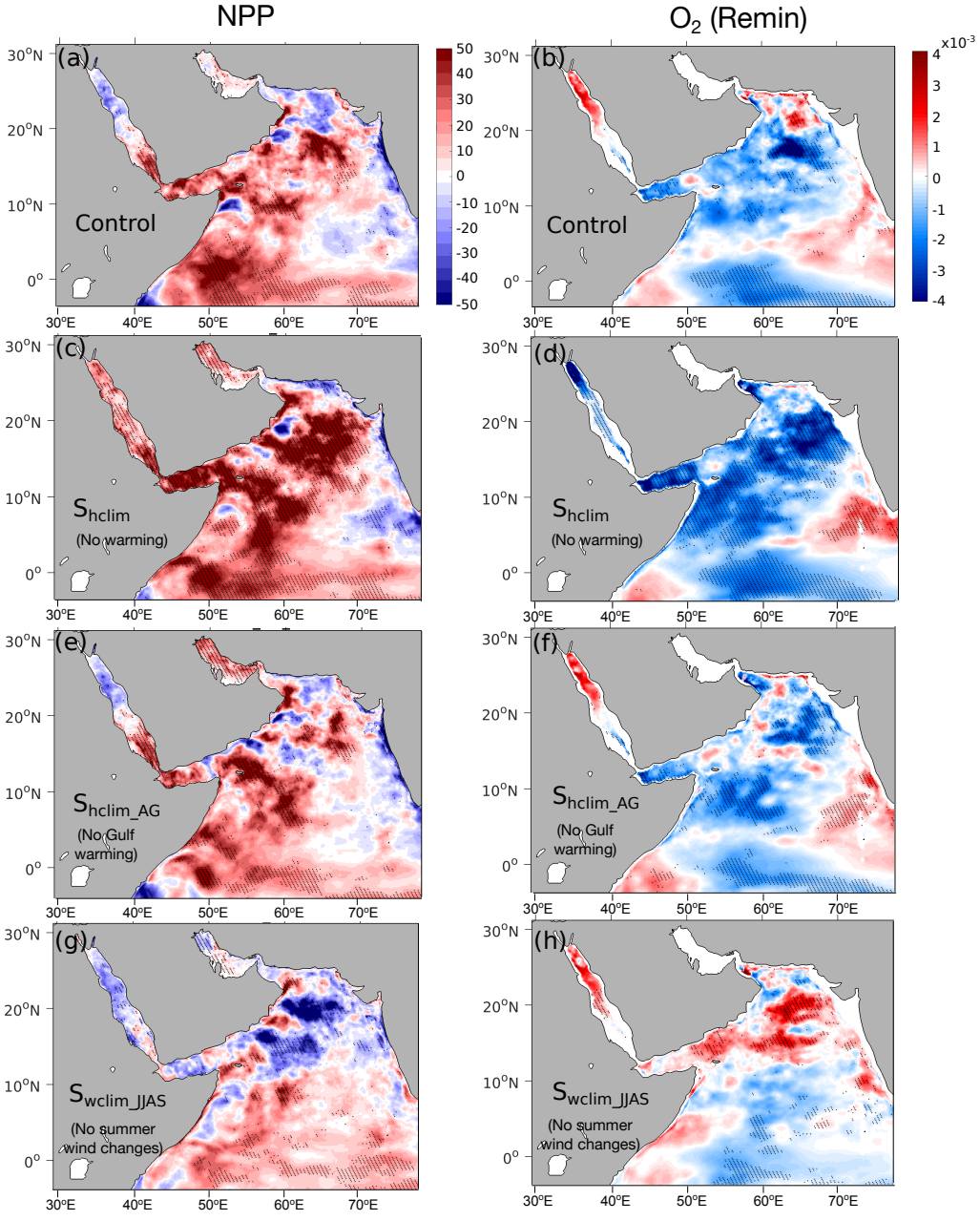

Figure 13. Net primary productivity and O_2 changes due to remineralization under different atmospheric forcing scenarios. Linear trends in (left) NPP (in mol m^{-2} yr^{-1} $decade^{-1}$) and (right) O_2 changes due to organic matter remineralization in the 200-1000 m layer (in mmol m^{-2} s^{-1} $decade^{-1}$) in the (a-b) control and (c-h) under different atmospheric forcing scenatios. Statistically significant trends at 95% confidence interval following a Mann-Kendall (MK) test are represented by hatching.

https://doi.org/10.5194/bg-2020-325
Preprint. Discussion started: 14 September 2020


Biogeosciences Discussions Open Access EGU

4.2 Comparison with previous works

The fact that recent subsurface deoxygenation in the northern AS has been mostly driven by reduced ventilation is consistent with previous results from Earth System models showing that tropical subsurface ocean O_2 changes projected for the twenty-first century and those simulated during the last deglaciation are more driven by changes in ventilation than biology (Bopp et al., 2017). Our analysis has revealed that summer monsoon wind increase over the study period has mostly caused upper ocean oxygenation (south of 20°N), and to a lesser extent has contributed to deoxygenation at depth (through enhanced O_2 consumption). This is consistent with the findings of Lachkar et al. (2018) who investigated the impacts of idealized perturbations in monsoon wind intensity on the size and intensity of the AS OMZ and found that the OMZ expands and deepens in response to monsoon wind intensification. Our finding that the suboxic volume and denitrification are highly sensitive to deoxygenation is consistent with previous studies that suggest high vulnerability of suboxic zones to small changes in the ocean's O_2 content. For instance, the world's largest suboxic zone in the Pacific Ocean was shown to vary in size by a factor two in model-based reconstructions of historical oxygen changes (Deutsch et al., 2011). Finally, the weaker sensitivity of the volume of hypoxia to deoxygneation in the AS is a consequence of the near compensation by wind-driven oxygenation trends in the central and eastern AS and is consistent with previous studies suggesting a generally weaker sensitivity of the hypoxic volume to deoxygenation. For instance, it was estimated that a decrease of the upper ocean O_2 concentration by 5 mmol m^{-3} could lead to a tripling of the suboxic volume and only 10% increase in the hypoxic volume (Deutsch et al., 2011).

4.3 Future deoxygenation in the AS

As the AS and the Gulf continue to warm under future climate change, deoxygenation may accelerate in the region. Modeling studies suggest indeed further ocean deoxygenation in the northern AS in the future. For instance, CMIP5 models project a drop of O_2 by up to 20 mmol m^{-3} in the Sea of Oman in the layer between 200 m and 600 m by the end of the century under the RCP8.5 emission scenario (Bopp et al., 2013). The CMIP6 multi-model ensemble average indicates an even stronger oxygen decline of more than 30 mmol m^{-3} by 2100, in the northern AS between 100 m and 600 m, essentially driven by an increase in the AOU (Kwiatkowski et al., 2020). These changes can have dramatic impacts on O_2-sensitive species and nitrogen and carbon cycling in the region. Furthermore, the impacts of these O_2 changes on marine ecosystems are likely to be exacerbated by concurrent stressors such as warming, declining productivity and ocean acidification. For instance, the fast warming of the AS upper ocean is likely to cause an increase in the metabolic rates. This in turn is expected to increase organisms oxygen demand at the same time where O_2 supply to the environment is dropping (Levin, 2018; Deutsch et al., 2015). Furthermore, oxygen-induced vertical plankton migration can intensify O_2 depletion at depth (Bianchi et al., 2013). It is also established that ocean acidification interacts with deoxygenation and can aggravate the effects of low oxygen on organisms (Gobler and Baumann, 2016; Miller et al., 2016).

https://doi.org/10.5194/bg-2020-325
Preprint. Discussion started: 14 September 2020

4.4 Caveats and limitations

Our study has a couple of caveats and limitations. Among the study's main limitations is the relatively short simulation period that precludes the attribution of the documented O_2 changes to climate change vs. natural variability. Previous observations suggest that the natural variability in O_2, dominated by interannual and decadal oscillations, can locally be stronger than the long-term trends associated with climate warming (Whitney et al., 2007; Cummins and Ross, 2020). Strong modulation of interrannual variability in hypoxic and suboxic volumes by decadal oscillations has been documented in previous studies (e.g., Deutsch et al., 2011, 2014). This complicates the detection and attribution of long-term responses to climate change. Therefore, it is not unlikely that an important fraction of the trends simulated here is associated with natural variability as it has been shown that the emergence of the climate change signal among the internal variability range is generally slow for oxygen, with only a small fraction of the ocean experiencing emergence before the end of the century (Frölicher et al., 2016). According to the same study, the earliest emergence of the O_2 signal in the AS is expected to occur only by the middle of the current century. Yet, according to other studies the emergence of the climate change signal from the noise of natural variability can occur as early as 2010 or 2020 in the ventilated thermocline of the northern AS (Long et al., 2016; Hameau et al., 2019).

Other study limitations pertain to the biogeochemical model assumptions. For instance, the lack of a representation of some major limiting nutrients such as iron, silicate and phosphate can potentially cause biases in regions where these nutrients contribute to limit biological production (e.g., off Somalia). However, previous studies suggest nitrogen is the main limiting nutrient in the Indian Ocean at larger scales (Koné et al., 2009). Other major model-related limitations concern the lack of representation of important biogeochemical processes such as N_2 fixation and the crude representation of microbial respiration in the model. Yet, on the one hand recent studies suggest that N_2 fixation has a limited effect on the AS OMZ as it constitutes only a negligible proportion of new nitrogen there (Guieu et al., 2019). On the other hand, simple representations of microbial respiration that miss potentially important biogeochemical feedbacks are a common problem in most existing biogeochemical models (Oschlies et al., 2018; Robinson, 2019). Additional work that combine expanding the current oxygen-measurement system and improving the complexity of microbial respiration in numerical models is needed to reduce biases in model estimates of deoxygenation (Oschlies et al., 2018).

5 Summary and Conclusions

We reconstruct the evolution of dissolved ocean in the AS from 1982 through 2010 using a series of hindcast simulations performed with an eddy-resolving ocean biogeochemical model forced with ERA atmospheric reanalysis. We find a significant thermocline deoxygenation in the northern and western AS, with the ocean O_2 content dropping by around 2% decade^{-1} and 7% decade^{-1} in the 0-200 m and the 200-1000 m, respectively. These changes are associated with a statistically significant increase of the volume of suboxia ($O_2 < 4$mmol m^{-3}) and denitrification by up to 30% around and 40% over the study period, respectively. Using a set of sensitivity simulations we demonstrate that deoxygenation in the northern AS has been caused essentially by a widespread warming of the sea surface, in particular in the Gulf, causing a reduction in the ventilation of the subsurface and intermediate layers. Additionally, we show that a concomitant summer monsoon intensification over the

https://doi.org/10.5194/bg-2020-325
Preprint. Discussion started: 14 September 2020

study period has enhanced the ventilation and hence the oxygenation of the upper ocean south of 20°N but has contributed to deoxygenation in the northern AS and at depth. This is because surface warming increases vertical stratification, thus reducing ventilation of the intermediate ocean, while summer monsoon wind intensification causes the thermocline depth to rise in the northern AS and deepen elsewhere, thus contributing to lowering O_2 levels in the upper 200 m in the northern AS and increasing it in the rest of the AS. Finally, wind change-driven enhanced productivity south of 20°N contributes to deoxygenation observed at depth in the western and central AS. Our findings confirm that the AS OMZ is strongly sensitive to upper-ocean warming and concurrent changes in the Indian monsoon winds. Our results also demonstrate that changes in the local climatic forcing play a key role in regional dissolved oxygen changes and hence need to be properly represented in global models to reduce uncertainties in future projections of deoxygenation.

Acknowledgements. Support for this research has come from the Center for Prototype Climate Modeling (CPCM), the New York University Abu Dhabi (NYUAD) Research Institute. Computations were performed at the High Performance cluster (HPC) of NYUAD, Dalma. We thank B. Marchand and M. Barwani from the NYUAD HPC team for technical support. The authors declare that they have no competing financial interests. The data used for forcing and validating the model are publicly available online and can be accessed from cited references. The model code can be accessed online at http://www.romsagrif.org.

https://doi.org/10.5194/bg-2020-325
Preprint. Discussion started: 14 September 2020

References

Al-Ansari, E. M., Rowe, G., Abdel-Moati, M., Yigiterhan, O., Al-Maslamani, I., Al-Yafei, M., Al-Shaikh, I., and Upstill-Goddard, R.: Hypoxia in the central Arabian Gulf Exclusive Economic Zone (EEZ) of Qatar during summer season, Estuarine, Coastal and Shelf Science, 159, 60–68, 2015.

Al-Rashidi, T. B., El-Gamily, H. I., Amos, C. L., and Rakha, K. A.: Sea surface temperature trends in Kuwait bay, Arabian Gulf, Natural Hazards, 50, 73–82, 2009.

Al-Yamani, F. and Naqvi, S.: Chemical oceanography of the Arabian Gulf, Deep Sea Research Part II: Topical Studies in Oceanography, 161, 72–80, 2019.

Bange, H. W., Naqvi, S. W. A., and Codispoti, L.: The nitrogen cycle in the Arabian Sea, Progress in Oceanography, 65, 145–158, 2005.

Banse, K., Naqvi, S., Narvekar, P., Postel, J., and Jayakumar, D.: Oxygen minimum zone of the open Arabian Sea: variability of oxygen and nitrite from daily to decadal timescales., Biogeosciences, 11, 2237–2261, 2014.

Barnier, B., Siefridt, L., and Marchesiello, P.: Thermal forcing for a global ocean circulation model using a three-year climatology of ECMWF analyses, Journal of Marine Systems, 6, 363–380, 1995.

Bianchi, D., Galbraith, E. D., Carozza, D. A., Mislan, K., and Stock, C. A.: Intensification of open-ocean oxygen depletion by vertically migrating animals, Nature Geoscience, 6, 545–548, 2013.

Bopp, L., Resplandy, L., Orr, J. C., Doney, S. C., Dunne, J. P., Gehlen, M., Halloran, P., Heinze, C., Ilyina, T., Seferian, R., et al.: Multiple stressors of ocean ecosystems in the 21st century: projections with CMIP5 models, Biogeosciences, 10, 6225–6245, 2013.

Bopp, L., Resplandy, L., Untersee, A., Le Mezo, P., and Kageyama, M.: Ocean (de) oxygenation from the Last Glacial Maximum to the twenty-first century: insights from Earth System models, Philosophical Transactions of the Royal Society A: Mathematical, Physical and Engineering Sciences, 375, 20160 323, 2017.

Breitburg, D., Levin, L. A., Oschlies, A., Grégoire, M., Chavez, F. P., Conley, D. J., Garçon, V., Gilbert, D., Gutiérrez, D., Isensee, K., et al.: Declining oxygen in the global ocean and coastal waters, Science, 359, 2018.

Bristow, L. A., Callbeck, C. M., Larsen, M., Altabet, M. A., Dekaezemacker, J., Forth, M., Gauns, M., Glud, R. N., Kuypers, M. M., Lavik, G., et al.: N 2 production rates limited by nitrite availability in the Bay of Bengal oxygen minimum zone, Nature Geoscience, 10, 24–29, 2017.

Burt, J. A., Paparella, F., Al-Mansoori, N., Al-Mansoori, A., and Al-Jailani, H.: Causes and consequences of the 2017 coral bleaching event in the southern Persian/Arabian Gulf, Coral Reefs, 38, 567–589, 2019.

Chaidez, V., Dreano, D., Agusti, S., Duarte, C. M., and Hoteit, I.: Decadal trends in Red Sea maximum surface temperature, Scientific Reports, 7, 1–8, 2017.

Cocco, V., Joos, F., Steinacher, M., Frölicher, T. L., Bopp, L., Dunne, J., Gehlen, M., Heinze, C., Orr, J., Oschlies, A., et al.: Oxygen and indicators of stress for marine life in multi-model global warming projections, Biogeosciences, 10, 1849–1868, 2013.

Codispoti, L., Brandes, J. A., Christensen, J., Devol, A., Naqvi, S., Paerl, H. W., and Yoshinari, T.: The oceanic fixed nitrogen and nitrous oxide budgets: Moving targets as we enter the anthropocene?, Scientia Marina, 65, 85–105, 2001.

Cummins, P. F. and Ross, T.: Secular trends in water properties at Station P in the northeast Pacific: an updated analysis, Progress in Oceanography, p. 102329, 2020.

Dai, A. and Trenberth, K. E.: Estimates of freshwater discharge from continents: Latitudinal and seasonal variations, Journal of hydrometeorology, 3, 660–687, 2002.

https://doi.org/10.5194/bg-2020-325
Preprint. Discussion started: 14 September 2020

Deutsch, C., Brix, H., Ito, T., Frenzel, H., and Thompson, L.: Climate-forced variability of ocean hypoxia, science, 333, 336–339, 2011.

Deutsch, C., Berelson, W., Thunell, R., Weber, T., Tems, C., McManus, J., Crusius, J., Ito, T., Baumgartner, T., Ferreira, V., et al.: Centennial changes in North Pacific anoxia linked to tropical trade winds, Science, 345, 665–668, 2014.

Deutsch, C., Ferrel, A., Seibel, B., Pörtner, H.-O., and Huey, R. B.: Climate change tightens a metabolic constraint on marine habitats, Science, 348, 1132–1135, 2015.

do Rosário Gomes, H., Goes, J. I., Matondkar, S. P., Buskey, E. J., Basu, S., Parab, S., and Thoppil, P.: Massive outbreaks of Noctiluca scintillans blooms in the Arabian Sea due to spread of hypoxia, Nature Communications, 5, 1–8, 2014.

Frölicher, T. L., Rodgers, K. B., Stock, C. A., and Cheung, W. W.: Sources of uncertainties in 21st century projections of potential ocean ecosystem stressors, Global Biogeochemical Cycles, 30, 1224–1243, 2016.

Garcia, H. E., Boyer, T. P., Locarnini, R. A., Antonov, J. I., Mishonov, A. V., Baranova, O. K., Zweng, M. M., Reagan, J. R., Johnson, D. R., and Levitus, S.: World ocean atlas 2013. Volume 3, Dissolved oxygen, apparent oxygen utilization, and oxygen saturation, 2013a.

Garcia, H. E., Locarnini, R. A., Boyer, T. P., Antonov, J. I., Baranova, O. K., Zweng, M. M., Reagan, J. R., Johnson, D. R., Mishonov, A. V., and Levitus, S.: World ocean atlas 2013. Volume 4, Dissolved inorganic nutrients (phosphate, nitrate, silicate), 2013b.

Gobler, C. J. and Baumann, H.: Hypoxia and acidification in ocean ecosystems: coupled dynamics and effects on marine life, Biology letters, 12, 20150 976, 2016.

Goes, J. I., Thoppil, P. G., do R Gomes, H., and Fasullo, J. T.: Warming of the Eurasian landmass is making the Arabian Sea more productive, Science, 308, 545–547, 2005.

Griffies, S. M., Danabasoglu, G., Durack, P. J., Adcroft, A. J., Balaji, V., Boning, C. W., Chassignet, E. P., Curchitser, E., Deshayes, J., Drange, H., et al.: OMIP contribution to CMIP6: experimental and diagnostic protocol for the physical component of the Ocean Model Intercomparison Project, Geoscientific Model Development, pp. 3231–3296, 2016.

Gruber, N., Frenzel, H., Doney, S. C., Marchesiello, P., McWilliams, J. C., Moisan, J. R., Oram, J. J., Plattner, G.-K., and Stolzenbach, K. D.: Eddy-resolving simulation of plankton ecosystem dynamics in the California Current System, Deep Sea Research Part I: Oceanographic Research Papers, 53, 1483–1516, 2006.

Guieu, C., Al Azhar, M., Aumont, O., Mahowald, N., Lévy, M., Éthé, C., and Lachkar, Z.: Major impact of dust deposition on the productivity of the Arabian Sea, Geophysical Research Letters, 46, 6736–6744, 2019.

Hameau, A., Mignot, J., and Joos, F.: Assessment of time of emergence of anthropogenic deoxygenation and warming: insights from a CESM simulation from 850 to 2100 CE, Biogeosciences, 16, 1755–1780, 2019.

Ito, T., Minobe, S., Long, M. C., and Deutsch, C.: Upper ocean O2 trends: 1958–2015, Geophysical Research Letters, 44, 4214–4223, 2017.

Kendall, M. G.: Rank correlation methods., 1948.

Koné, V., Aumont, O., Lévy, M., and Resplandy, L.: Physical and biogeochemical controls of the phytoplankton seasonal cycle in the Indian Ocean: A modeling study, Indian Ocean Biogeochemical Processes and Ecological Variability, 185, 350, 2009.

Krishna, M., Prasad, M., Rao, D., Viswanadham, R., Sarma, V., and Reddy, N.: Export of dissolved inorganic nutrients to the northern Indian Ocean from the Indian monsoonal rivers during discharge period, Geochimica et Cosmochimica Acta, 172, 430–443, 2016.

Kumar, S. P., Roshin, R. P., Narvekar, J., Kumar, P. D., and Vivekanandan, E.: Response of the Arabian Sea to global warming and associated regional climate shift, Marine Environmental Research, 68, 217–222, 2009.

Kwiatkowski, L., Torres, O., Bopp, L., Aumont, O., Chamberlain, M., Christian, J. R., Dunne, J. P., Gehlen, M., Ilyina, T., John, J. G., et al.: Twenty-first century ocean warming, acidification, deoxygenation, and upper-ocean nutrient and primary production decline from CMIP6 model projections, Biogeosciences, 17, 3439–3470, 2020.

https://doi.org/10.5194/bg-2020-325
Preprint. Discussion started: 14 September 2020

Lachkar, Z., Smith, S., Lévy, M., and Pauluis, O.: Eddies reduce denitrification and compress habitats in the Arabian Sea, Geophysical Research Letters, 43, 9148–9156, 2016.

Lachkar, Z., Lévy, M., and Smith, S.: Intensification and deepening of the Arabian Sea oxygen minimum zone in response to increase in Indian monsoon wind intensity., Biogeosciences, 15, 2018.

Lachkar, Z., Lévy, M., and Smith, K.: Strong intensification of the Arabian Sea oxygen minimum zone in response to Arabian Gulf warming, Geophysical Research Letters, 46, 5420–5429, 2019.

Laffoley, D. D. and Baxter, J.: Ocean Deoxygenation: Everyone's Problem-Causes, Impacts, Consequences and Solutions, IUCN, 2019.

Large, W. G., McWilliams, J. C., and Doney, S. C.: Oceanic vertical mixing: A review and a model with a nonlocal boundary layer parameterization, Reviews of Geophysics, 32, 363–403, 1994.

Levin, L. A.: Manifestation, drivers, and emergence of open ocean deoxygenation, Annual review of marine science, 10, 229–260, 2018.

Long, M. C., Deutsch, C., and Ito, T.: Finding forced trends in oceanic oxygen, Global Biogeochemical Cycles, 30, 381–397, 2016.

Lumpkin, R. and Johnson, G. C.: Global ocean surface velocities from drifters: Mean, variance, El Niño–Southern Oscillation response, and seasonal cycle, Journal of Geophysical Research: Oceans, 118, 2992–3006, 2013.

Mann, H. B.: Nonparametric tests against trend, Econometrica: Journal of the econometric society, pp. 245–259, 1945.

Marchesiello, P., Debreu, L., and Couvelard, X.: Spurious diapycnal mixing in terrain-following coordinate models: The problem and a solution, Ocean Modelling, 26, 156–169, 2009.

Miller, S. H., Breitburg, D. L., Burrell, R. B., and Keppel, A. G.: Acidification increases sensitivity to hypoxia in important forage fishes, Marine Ecology Progress Series, 549, 1–8, 2016.

Oschlies, A., Brandt, P., Stramma, L., and Schmidtko, S.: Drivers and mechanisms of ocean deoxygenation, Nature Geoscience, 11, 467–473, 2018.

Parvathi, V., Suresh, I., Lengaigne, M., Izumo, T., and Vialard, J.: Robust projected weakening of winter monsoon winds over the Arabian Sea under climate change, Geophysical Research Letters, 44, 9833–9843, 2017.

Piontkovski, S. and Al-Oufi, H.: The Omani shelf hypoxia and the warming Arabian Sea, International Journal of Environmental Studies, 72, 256–264, 2015.

Queste, B. Y., Vic, C., Heywood, K. J., and Piontkovski, S. A.: Physical controls on oxygen distribution and denitrification potential in the north west Arabian Sea, Geophysical Research Letters, 45, 4143–4152, 2018.

Rabalais, N. N., Turner, R. E., and Wiseman Jr, W. J.: Gulf of Mexico hypoxia, aka "The dead zone", Annual Review of ecology and Systematics, 33, 235–263, 2002.

Ramesh, R., Purvaja, G., and Subramanian, V.: Carbon and phosphorus transport by the major Indian rivers, Journal of Biogeography, pp. 409–415, 1995.

Robinson, C.: Microbial respiration, the engine of ocean deoxygenation, Frontiers in Marine Science, 5, 533, 2019.

Roxy, M. K., Modi, A., Murtugudde, R., Valsala, V., Panickal, S., Prasanna Kumar, S., Ravichandran, M., Vichi, M., and Lévy, M.: A reduction in marine primary productivity driven by rapid warming over the tropical Indian Ocean, Geophysical Research Letters, 43, 826–833, 2016.

Schmidtko, S., Stramma, L., and Visbeck, M.: Decline in global oceanic oxygen content during the past five decades, Nature, 542, 335–339, 2017.

Schott, F. A., Xie, S.-P., and McCreary Jr, J. P.: Indian Ocean circulation and climate variability, Reviews of Geophysics, 47, 2009.

https://doi.org/10.5194/bg-2020-325
Preprint. Discussion started: 14 September 2020

Séférian, R., Berthet, S., Yool, A., Palmiéri, J., Bopp, L., Tagliabue, A., Kwiatkowski, L., Aumont, O., et al.: Tracking improvement in simulated marine biogeochemistry between CMIP5 and CMIP6, Current Climate Change Reports, 10, 2020.

Shchepetkin, A. F. and McWilliams, J. C.: The regional oceanic modeling system (ROMS): a split-explicit, free-surface, topography-following-coordinate oceanic model, Ocean modelling, 9, 347–404, 2005.

Stramma, L., Johnson, G. C., Sprintall, J., and Mohrholz, V.: Expanding oxygen-minimum zones in the tropical oceans, science, 320, 655–658, 2008.

Strong, A. E., Liu, G., Skirving, W., and Eakin, C. M.: NOAA's Coral Reef Watch program from satellite observations, Annals of GIS, 17, 83–92, 2011.

Taylor, K. E.: Summarizing multiple aspects of model performance in a single diagram, Journal of Geophysical Research: Atmospheres, 106, 7183–7192, 2001.

Vaquer-Sunyer, R. and Duarte, C. M.: Thresholds of hypoxia for marine biodiversity, Proceedings of the National Academy of Sciences, 105, 15 452–15 457, 2008.

Wang, B., Liu, J., Kim, H.-J., Webster, P. J., Yim, S.-Y., and Xiang, B.: Northern Hemisphere summer monsoon intensified by mega-El Niño/southern oscillation and Atlantic multidecadal oscillation, Proceedings of the National Academy of Sciences, 110, 5347–5352, 2013.

Whitney, F. A., Freeland, H. J., and Robert, M.: Persistently declining oxygen levels in the interior waters of the eastern subarctic Pacific, Progress in Oceanography, 75, 179–199, 2007.